ORIGINAL PAPER

Caspase-3 feeds back on caspase-8, Bid and XIAP in type I Fas signaling in primary mouse hepatocytes

Karine Sá Ferreira · Clemens Kreutz ·
Sabine MacNelly · Karin Neubert · Angelika Haber ·
Matthew Bogyo · Jens Timmer · Christoph Borner

Abstract The TNF-R1 like receptor Fas is highly expressed on the plasma membrane of hepatocytes and plays an essential role in liver homeostasis. We recently showed that in collagen-cultured primary mouse hepatocytes, Fas stimulation triggers apoptosis via the so-called type I extrinsic signaling pathway. Central to this pathway is the direct caspase-8-mediated cleavage and activation of caspase-3 as compared to the type II pathway which first requires caspase-8-mediated Bid cleavage to trigger mitochondrial cytochrome *c* release for caspase-3 activation. Mathematical modeling can be used to understand complex signaling systems such as crosstalks and feedback or feedforward loops. A previously published model predicted a positive feedback loop between active caspases-3 and -8 in both type I and type II FasL signaling in lymphocytes and Hela cells, respectively. Here we experimentally tested this hypothesis in our hepatocytic type I Fas signaling pathway by using wild-type and XIAP-deficient primary hepatocytes and two recently characterized, selective caspase-3/-7 inhibitors (AB06 and AB13). Caspase-3/-7 activity assays and quantitative western blotting confirmed that fully processed, active p17 caspase-3 feeds back on caspase-8 by cleaving its partially processed p43 form into the fully processed p18 species. Our data do not discriminate if p18 positively or negatively influences FasL-induced apoptosis or is responsible for non-apoptotic aspects of FasL signaling. However, we found that caspase-3 also feeds back on Bid and degrades its own inhibitor XIAP, both events that may enhance caspase-3 activity and apoptosis. Thus, potent, selective caspase-3 inhibitors are useful tools to understand complex signaling circuitries in apoptosis.

K. S. Ferreira · K. Neubert · A. Haber · C. Borner (✉)
Institute of Molecular Medicine and Cell Research, University of Freiburg, Stefan-Meier-Str. 17, 79104 Freiburg, Germany
e-mail: christoph.borner@uniklinik-freiburg.de

K. S. Ferreira · C. Borner
GRK 1104, From Cells to Organs: Molecular Mechanisms of Organogenesis, Faculty of Biology, University of Freiburg, Schaenzlestr. 1, 79104 Freiburg, Germany

C. Kreutz · J. Timmer
Institute for Physics, University of Freiburg, Hermann-Herder-Str. 3, 79104 Freiburg, Germany

C. Kreutz · J. Timmer
Freiburg Center for Systems Biology (ZBSA), University of Freiburg, Habsburgerstr. 49, 79104 Freiburg, Germany

S. MacNelly
Internal Medicine, University Hospital of Freiburg, Hugstetterstr. 55, 79106 Freiburg, Germany

M. Bogyo
Department of Pathology, School of Medicine, Stanford University, 300 Pasteur Drive, Stanford, CA 94305, USA

J. Timmer
Freiburg Institute for Advanced Studies (FRIAS), University of Freiburg, Albertstr. 19, 79104 Freiburg, Germany

J. Timmer · C. Borner
BIOSS Centre for Biological Signalling Studies, University of Freiburg, Hebelstr. 25, 79104 Freiburg, Germany

J. Timmer
Department of Clinical and Experimental Medicine, Linköping University, Universitetssjukhuset, 581 85 Linköping, Sweden

C. Borner
Spemann Graduate School of Biology and Medicine (SGBM), University of Freiburg, Albertstrasse 19A, 79104 Freiburg, Germany

Abbreviations

BAR	Bifunctional apoptosis regulator
DIABLO	Direct IAP-binding protein
DISC	Death-inducing signaling complex
FasL	Fas ligand
N2A FasL	Multimerised FasL obtained from stably transfected Neuro2A cells
PARP	Poly ADP ribose polymerase
Q-VD-OPh	Quinolyl-valyl-*O*-methylaspartyl-[-2,6-difluorophenoxy]-methylketon
Smac	Second mitochondrial-derived activator of caspase
wt	Wild-type
XIAP	X-chromosome-linked IAP (inhibitor of apoptosis protein)

Introduction

Cell death is an essential process for multicellular organisms as it is crucial for their proper embryonic development and tissue homeostasis in the adult [1]. High amounts of Fas, a member of the tumor necrosis factor (TNF) receptor superfamily also known as CD95, are constitutively expressed on the surface of hepatocytes [2, 3]. In the liver, Fas plays an important role during viral and autoimmune hepatitis, alcoholic liver disease and endotoxin- or ischemia/reperfusion-induced liver damage with the possible development of liver cirrhosis or hepatic carcinoma [2, 4–7]. Indeed, mice injected with an agonistic Fas antibody show extensive liver apoptosis and die rapidly from fulminant hepatitis [3, 8, 9].

After Fas ligand (FasL) binds to Fas on the surface, two apoptotic signaling cascades can be initiated, a direct type I pathway and a mitochondria mediated type II pathway [10]. Both pathways start with the formation of the death inducing signaling complex (DISC) at the activated Fas receptor [11]. Following conformational change after FasL binding, the intracellular domain of Fas is able to bind to the adaptor FADD which in turn recruits from the cytosol two monomeric initiator procaspase-8a (p55) or -8b (p53) molecules into close proximity [12–14]. This proximity allows the p55 and p53 proforms of caspase-8 to be autoprocessed into their respective p43/p12 and p41/p10 tetrameric active forms. The tetrameric forms stay associated with the DISC and then either cleave the BH3-only protein Bid (type II pathway) [8, 9, 15] or directly process the p32 proform of caspase-3 to a partially active p19/p12, and through further autoprocessing, to a highly active p17/p12 tetrameric caspase-3 enzyme (type I pathway) [10, 11, 16]. In the type II pathway cleaved Bid (tBid) migrates to mitochondria where it activates Bax/Bak leading to increased mitochondrial membrane permeability (MOMP) and the consequent release of cytochrome *c* [17]. Cytochrome *c* forms with the adapter Apaf-1 and the initiator caspase-9 a heptameric holoenzyme complex, called the apoptosome, which in turn processes the p32 proform of caspase-3 into the same p19/p12 and p17/p12 active tetrameric caspase-3 enzymes.

Interestingly, at least in lymphocytes and hepatocytes, Fas signaling not only triggers apoptosis but also proliferation [16]. This response seems to be crucial for liver regeneration as it is reduced in Fas mutant/lpr mice after partial hepatectomy [18]. Perplexingly, the mitogenic signaling induced by Fas also depends on caspase-8 [19, 20]. Moreover, caspase-8 has been implicated in macrophage differentiation [19], tumor cell migration [21] and skin protection from inflammatory reactions [22]. How the enzyme switches between apoptotic and non-apoptotic events has not yet been clearly defined. Recent evidence from knock-in mice carrying cleavage mutants of caspase-8 suggested that the processing of p55 or p53 pro-caspase-8 into p43/p12 or p41/p10 complexes is required for apoptosis, but not for non-apoptotic processes [20].

Although p43/p12 and p41/p10 tetrameric caspase-8 complexes are thought to be fully active at the DISC and to exhibit a broad substrate repertoire [23–25], both complexes can be further processed to catalytically inactive p26 or p24 fragments, which stay at the DISC, and a catalytically active p18 form which is released into the cytosol and forms with the p12 caspase-8a and p10 caspase-8b subunits two soluble p18/p12 and p18/p10 tetrameric enzyme complexes [24]. The role of these p18 caspase-8 complexes in the cytosol is still debated. It is assumed that they can further cleave Bid and pro-caspase-3 to enhance type II and I apoptosis signaling [11, 16]. However, recent experimental evidence indicated that the formation of p18 may rather downregulate or restrict Fas signaling because cleavage mutants of caspase-8 which could not be processed to p18 (D210A/D216A), and hence accumulated as p43 or p41 complexes, exhibited enhanced apoptosis as compared to wild-type caspase-8 [24, 26].

In type II Fas signaling it was reported that active caspase-3 can cleave its initiator caspases-9 and -8 [27, 28]. This feedback mechanism was considered to occur via the intermediate processing and activation of caspase-6 [29, 30] and thought to be a positive feedback mechanism to further enhance apoptosis through mitochondria and caspase-3 activation. A mathematical model developed by

Eissing et al. [31] predicted bistability and a positive feedback loop between caspase-3 and caspase-8 in type I FasL signaling in SKW6.4 lymphocytes and type II FasL signaling in Hela cells. Bistability is considered to be a salient feature of cells which theoretically are either in the stable state of life or death. To ensure a bistable system a positive or double negative feedback loop is required [32, 33]. In the case of FasL signaling this could be represented by further caspase-8 activation via active caspase-3. It has already been shown by mathematical modeling that XIAP, as an inhibitor of both caspase-3 and caspase-9, triggers a positive feedback loop because cleaved caspase-3 sequesters XIAP away from caspase-9. This brings about bistability of the mitochondrial pathway [34]. In addition, positive feedback can be achieved through the caspase-3 mediated cleavage of Bid [35, 36].

In this study we wanted to obtain experimental evidence for the existence and the possible biological significance of a caspase-3 to -8 feedback loop in the type I FasL signaling of primary hepatocytes. We recently showed that primary mouse hepatocytes cultured on a collagen I monolayer died in a type I manner in response to Fas stimulation, whereas in the liver in vivo and in freshly isolated suspension cells, the death was Bid-dependent, hence type II [37]. So far unequivocal experimental proof of the caspase-3 to -8 feedback has been missing due to the lack of appropriate experimental tools. The use of pan-caspase inhibitors such as ZVAD or Q-VD-OPh (quinolyl-valyl-*O*-methylaspartyl-[-2,6-difluorophenoxy]-methylketone) and some caspase knock-out cell lines did not give a definitive answer because general inhibitors also block initial caspase-8 processing, and other caspases could be redundant in the feedback signaling. Here we used two novel selective and potent caspase-3/-7 inhibitors AB06 and AB13 [38], as well as wild-type and XIAP knock-out primary hepatocytes to show that the formation of p18 caspase-8 largely depends on active caspase-3 and therefore constitutes a feedback mechanism. Although we could not uncover the significance of this process, it is most likely not a positive feedback loop. A positive feedback is rather achieved through caspase-3 mediated downregulation of its major inhibitor XIAP and eventually Bid cleavage.

Experimental procedures

Isolation and cultivation of primary mouse hepatocytes

Primary mouse hepatocytes were isolated from 6 to 12 weeks old wild-type and XIAP knock-out C57BL/6 mice (Jackson Laboratories) based on the collagenase perfusion technique [39]. The isolated hepatocytes were plated on collagen I-coated 6-well plates containing William's medium E (WME) supplemented with 10% FCS, 100 nM dexamethasone, 2 mM L-glutamine and 1% penicillin/streptomycin solution (complete WME, Biochrom). After 4 h of adherence, the cells were washed twice in PBS and incubated overnight in complete WME without dexamethasone in a 5% CO_2 incubator at 37°C before treatment with FasL.

Collagen coating

6-well plates were incubated with 1 ml of collagen I (4.5 mg/ml) per well for 30 min at 37°C, diluted 1:10 in PBS. The collagen solution was removed before seeding the cells.

Source of FasL

Neuro2A cells stably transfected with a mouse FasL expression vector secreting FasL in a multimerized, exosomal form (N2A FasL) were kindly provided by Dr. Adriano Fontana, University Clinic Zurich, Switzerland [40]. The cell supernatants were collected and prepared for apoptosis induction as previously described [37].

Caspase-3/-7 specific inhibitors (AB06 and AB13)

AB06 and AB13 are irreversible caspase inhibitors containing an acyloxymethyl ketone (AOMK) reactive group that covalently modifies the active site cysteine of caspase-3 (and -7) and thereby prevents the autocatalysis of p19 caspase-3 to the highly active p17 fragment as well as the cleavage of classical caspase-3 substrates such as PARP [38]. They were synthesized according to published methods [38]. 1 µM of these inhibitors (diluted in DMSO) was used to block Fas-induced apoptosis in hepatocytes. As a comparison 25 µM of the pan-caspase inhibitor Q-VD-OPh (MP Biomedicals Europe, Illkirch, France) was used.

Visual documentation

Cells were photographed under the microscope Axiovert™ (Zeiss, Jena, Germany) after treatment with N2A FasL in the presence or absence of caspase inhibitors. Images were processed with the AxioVision™ software (Zeiss, Jena, Germany). Magnification was 400×.

Antibodies and reagents

Rabbit polyclonal anti-caspase-3 antibodies detecting the p32 proform (9661) and the p17 active form (9662) were obtained from Cell Signaling (diluted 1:500), rat monoclonal anti-caspase-8 (1G12) from Alexis (diluted 1:500), mouse monoclonal anti-XIAP (2F1) from Assay Designs

(diluted 1:1,000), rabbit polyclonal anti-PARP from Cell Signaling (diluted 1:1,000), rabbit polyclonal anti-ERK (9102) from Cell Signaling (diluted 1:1,000) and mouse monoclonal anti-beta actin (C4) from MP Biomedical (diluted 1:40,000). The rat monoclonal anti-Bid antibodies were a kind gift from David Huang, WEHI, Australia (diluted 1:700). Secondary horseradish peroxide-conjugated goat anti-rabbit and anti-mouse were purchased from Jackson Immuno Research Laboratories and peroxide-conjugated rabbit anti-rat (A5795) was purchased from Sigma (diluted 1:5,000).

Preparation of whole cell lysates

At selected time points, hepatocytes treated or not with N2AFasL in the presence or absence of AB06 or AB13 were washed in ice-cold PBS and lysed on-plate in ice-cold lysis buffer containing 20 mM Tris–HCl pH 7.5, 150 mM NaCl, 5 mM EDTA, pH 8.0, 5 mM sodium pyrophosphate, 1 mM sodium vanadate, 20 mM sodium phosphate pH 7.6 and 1% Triton-X, supplemented with protease and proteasome inhibitors (20 μg/ml aprotinin, 20 μg/ml leupeptin, 400 ng/ml pepstatin, 10 μg/ml cytochalasin B, 200 μM PMSF and 8 μM MG132). The lysate was centrifuged at $16,000 \times g$, 4°C for 5 min and the supernatant was used for DEVDase (caspase-3/-7) activity assays, determination of protein concentration (BCA method) and western blotting.

DEVDase activity assay

Caspase-3/-7 (DEVDase) activity was measured by incubating the protein extracts with 60 μM fluorogenic DEVD-AMC in a buffer (100 mM Hepes–KOH, pH 7.5) containing 10 mM DTT for 30 min at 37°C. Fluorescence was detected in the Fluoroskan Ascent™ equipment (Thermo Labsystems™) and the RFUs (relative fluorescence units) were normalized according to the protein concentration.

SDS-PAGE and western blot analysis

Equal protein amounts (60–100 μg) were electrophoresed on 10 and 15% gels (SDS-PAGE), transferred to nitrocellulose membranes, probed with different antibodies and visualized by enhanced chemiluminescence (PIERCE) as recommended by the supplier.

Quantification of western blots

Caspase-3, caspase-8, Bid, PARP and XIAP bands detected after ECL western blotting of wild-type and XIAP knock-out extracts were quantified by measuring the maximal luminescence intensities as Boehringer light units (BLUs) with the Lumi Imager™ equipment (Roche).

The unit "BLU" represents an absolute factor for the light intensity. Maximal BLU values were divided by the BLU values of the correspondent loading control (ERK or beta-actin).

Data analysis

Because the measurement noise shows neither a pure normal nor a pure log-normal distribution, an asinh-transformation was applied to the raw data as a preprocessing step. The asinh-transformation $\mathrm{asinh}(x) = \log [x + \mathrm{sqrt}(x^2 + 1)]$ has been suggested for cases in which the noise has normal and log-normal error components [41]. After transformation, the residuals were in good agreement with a normal distribution according to qq-plots and Kolmogorov–Smirnov tests, which have been calculated for each measured protein. Independently on the choice of data transformations, we discovered systematic errors between the measurements obtained from different cell preparations, i.e., the time course replicates measured for the same treatment showed the same dynamics but at different intensity levels. To adjust for this effect, the time course replicates were normalized to the same average before the means and the standard errors (SE) of individual time points were calculated. For plotting the dynamics induced by the stimulation, the final values were shifted to a common initial data point ($t_0 = 0$).

Results

Specific caspase-3 inhibitors effectively block type I Fas-induced apoptosis of primary mouse hepatocytes

When primary hepatocytes isolated from wild-type (wt) and XIAP knock-out (XIAP $^{-/-}$) mice plated on collagen I were treated with 100 ng/ml N2A FasL, they showed typical hallmarks of apoptosis such as loss of cell–cell contact, cell shrinkage and membrane blebbing (Fig. 1a) as well as increased caspase-3/-7 activity (Fig. 1b). As expected, morphological apoptosis (Fig. 1a) and caspase-3/-7 activity (Fig. 1b) were much higher in XIAP$^{-/-}$ cells. Interestingly, the kinetic pattern of caspase-3/-7 activation was similar between wt and XIAP$^{-/-}$ cells (Fig. 1b) indicating that increased caspase-3/-7 activity was due to the removal of a crucial caspase-3 inhibitor (XIAP) and not due to the elimination of a blockage upstream of caspase-3. Conversely, the concomitant addition of either 1 μM AB06 or AB13 completely prevented the apoptotic morphology (Fig. 1a) as well as caspase-3/-7 activation (Fig. 1b) in both FasL-treated wt and XIAP$^{-/-}$ cells. The inhibitors alone did not have any effect on the cell morphology (Fig. 1a, mock + AB06 and mock + AB13).
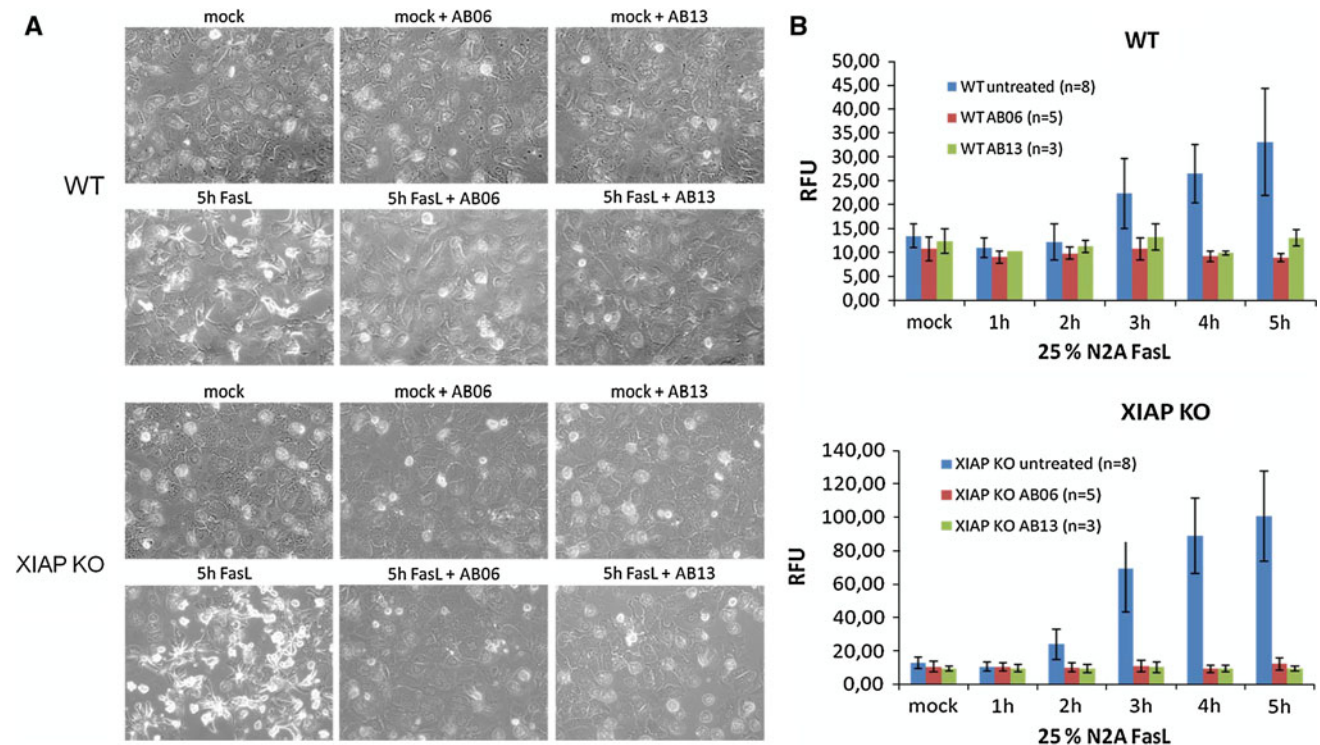
Fig. 1 The caspase-3/-7 inhibitors AB06 and AB13 inhibit FasL-induced apoptotic morphology and caspase-3/-7 activation. **a** Morphological examination and **b** caspase-3/-7 enzymatic activity (DEVDase assay) of wt and XIAP$^{-/-}$ (KO) primary mouse hepatocytes challenged with 100 ng/ml N2A FasL in the presence or absence of 1 μM of the caspase-3/-7 inhibitors AB06 or AB13; mock means untreated with FasL. The *values* are shown in relative fluorescence units (RFU). The data in **b** are the means of at least three independent experiments (n) $\pm$ SEM, $p < 0.02$. Please note that ordinates for XIAP KO are higher than for wt

This finding indicates that, at the concentrations chosen, AB06 and AB13 were effective caspase-3/-7 inhibitors in our system as they not only blocked apoptosis in wt but also in XIAP$^{-/-}$ cells where caspase-3/-7 activity was around four times higher (Fig. 1b—note that the ordinates for XIAP KO are approximately threefold higher than for wt). Their potency was also similar to that of the pan-caspase inhibitor QVD-OPh (Suppl. Fig. 1A). However, QVD-OPh not only blocked the processing and activation of caspase-3 but also that of caspase-8 and its substrate Bid (Suppl. Fig. 1B).

AB06 effectively blocks PARP cleavage and XIAP degradation by inhibiting the autoprocessing of p19 to p17 and the catalytic activity of p17 caspase-3

Concomitant with elevated caspase-3/-7 activity, we observed an effective processing of the p32 proform of caspase-3 into its active p19 and p17 fragments in FasL-treated wild-type hepatocytes (Fig. 2a). While in the first 2 h only p19 was formed due to caspase-8 mediated cleavage between the large and small subunit of caspase-3, thereafter p19 was gradually autoprocessed to the highly active p17 fragment. The auto-processing was completely inhibited by AB06 indicating that

this inhibitor fully blocked the autocatalytic activity of p19 caspase-3 (Fig. 2a). This was less pronounced with AB13, as some p17 was still formed from p19. Indeed, the covalent interaction of AB06 with p19 shifted the band up (see "+" in Fig. 2a), meaning that the p19 enzyme was fully blocked by the inhibitor. By contrast, with AB13, it was not p19, but p17, which shifted up (see "*" in Fig. 2a). Thus, autoproteolysis was still proceeding with AB13, but the enzymatic activity of p17 was blocked. Consistent with this notion, proteolysis of PARP, a classical caspase-3 substrate was entirely prevented by the caspase-3/-7 inhibitor AB06 and drastically diminished by AB13 (Fig. 2a). Importantly, the inhibitors were specific for caspase-3 (and also for caspase-7 which was not tested here) and did not affect caspase-8 activity as the processing of p32 procaspase-3 to p19 occurred at similar kinetics between inhibitor treated and untreated cells (Fig. 2a).

In XIAP$^{-/-}$ hepatocytes, the kinetic of p32 cleavage to p19 was similar to that in wt cells (Fig. 2a, lower panels) indicating that this caspase-8 mediated step was not affected by the lack of XIAP and the higher caspase-3 activity. By contrast, p19 caspase-3 was more rapidly converted to p17, and PARP cleavage occurred earlier and more extensively due to the higher caspase-3/-7 activity in XIAP$^{-/-}$ cells (Fig. 2a, lower panels). Again whereas
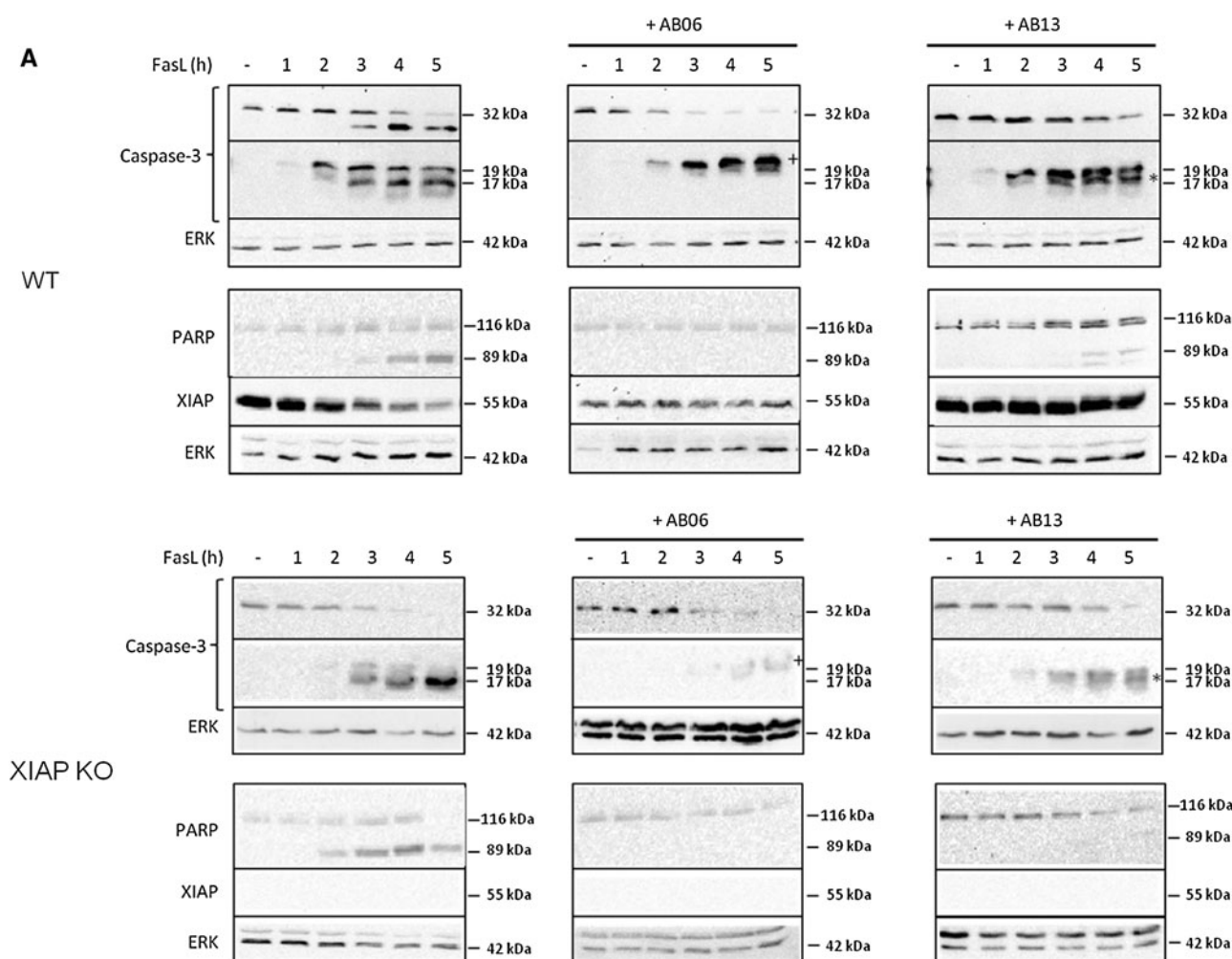
Fig. 2 Autoprocessing of p19 to p17 caspase-3, PARP cleavage and XIAP degradation are entirely blocked by AB06, autoprocessing only partially by AB13. **a** Anti-caspase-3, -PARP and -XIAP western blots of whole cell lysates of wt and XIAP$^{-/-}$ (KO) primary mouse hepatocytes challenged with 100 ng/ml N2A FasL in the absence or presence of 1 μM of the caspase-3 AB06 or AB13 for up to 5 h. 42 kDa ERK served as loading control. The molecular masses of the respective protein bands are indicated on the right of the blots. Note that in the presence of AB06 the p19 caspase-3 band slightly shifts up due to the covalent interaction of the inhibitor with the catalytic pocket of the enzyme (marked with "+"). The same happens for the p17 caspase-3 band with AB13 (marked with "*"). Light intensity quantification of **b** the p32, p19 and p17 caspase-3 (C3) and **c** the p55 XIAP and p89 PARP bands from 3 to 8 independent experiments (*n*) of which one is represented in **a**. Values are depicted in Boehringer light units (BLU). The data were processed by asinh-transformation, normalized to the same average and shifted to a common initial data point ($t_0 = 0$) as described in "Experimental procedures". The mean of at least three independent experiments is shown with standard errors. Please note that ordinates for wt and XIAP KO are not the same

AB06 blocked both the p19 to p17 conversion and PARP cleavage, AB13 did not fully inhibit these processes. Interestingly, FasL induced the degradation of XIAP which was fully blocked by both AB06 and AB13 (Fig. 2a). Thus, in type I Fas signaling, caspase-3 seems to degrade its own inhibitor which constitutes a positive feedback loop.

To obtain reproducible data of our finding, we quantified the maximal luminescence intensities of western blot bands from 3 to 8 independent experiments in a Lumi Imager^{TM} and normalized the data against the loading control of p42 ERK using the Lumi Analist^{TM} software. Figure 2b and c show the average luminescence of these analyses in so-called Boehringer Light Units (BLUs) with respective standard errors as described in "Experimental procedures". The untreated samples of all experiments were normalized to zero ($t_0 = 0$). In general, the quantified data obtained from these many experiments corroborated the qualitative findings shown in Fig. 2a. After FasL stimulation, the kinetics of p32 procaspase-3 disappearance and formation of its first p19 cleavage fragment were similar between caspase-inhibitor treated or untreated wt and XIAP$^{-/-}$ cells (Fig. 2b). However, the autoprocessing of p19 to the fully active p17 form was more
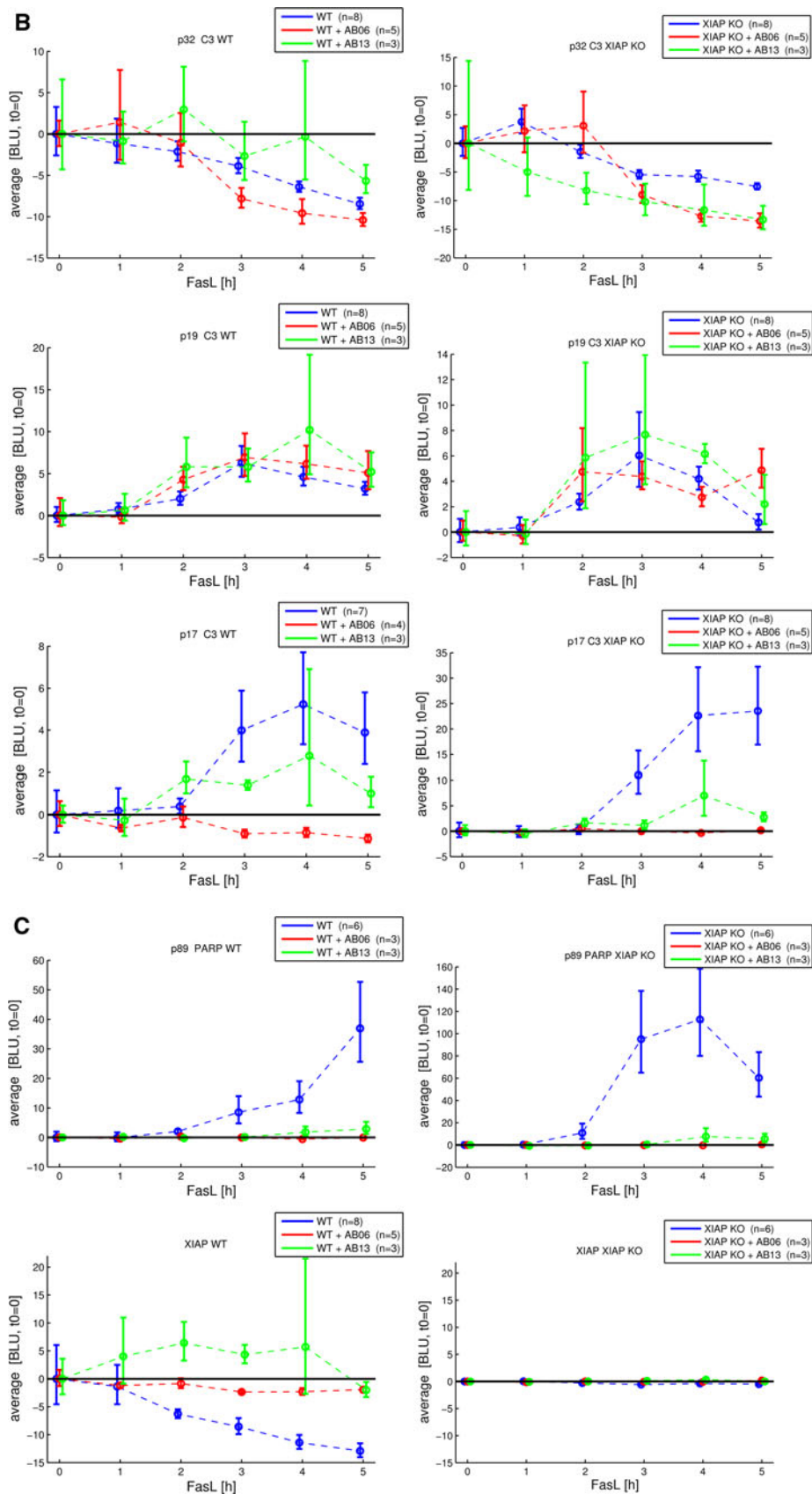
Fig. 2 continued

pronounced in XIAP$^{-/-}$ than wt cells (compare scales in Fig. 2b) and entirely prevented by AB06 in both. Again AB13 still allowed the formation of some p17. But consistent with the blockage of p17 caspase-3 activity by both AB06 and AB13, the cleavage of PARP into its p86 fragment was significantly impaired upon inhibitor treatment of FasL-stimulated wt and XIAP$^{-/-}$ hepatocytes (Fig. 2c). Moreover, AB06 and AB13 were similarly effective in blocking FasL-induced XIAP degradation (Fig. 2c).

Thus our data show that AB06 is a potent, selective caspase-3/-7 inhibitor that blocks all aspects of the caspase-3 enzyme (p19 to p17 autoprocessing, PARP cleavage and XIAP degradation). AB13 is less potent in inhibiting p19 to p17 caspase-3 autoprocessing but effectively blocks PARP cleavage and XIAP degradation (hence p17 activity) as well.

XIAP$^{-/-}$ cells and AB06/AB13 treatments reveal a caspase-3 to caspase-8 feedback loop after FasL stimulation

To monitor the processing and activation of caspase-8 in response to FasL treatment, we determined the kinetics of

formation of p43 or p41 and p18 fragments in wt and XIAP$^{-/-}$ cells in the presence or absence of AB06 and AB13 by anti-caspase-8 western blotting. As primary hepatocytes express only one procaspase-8 isoform (p55 or p53), we refer here to caspase-8 forms as p55, p43 and p18. The smaller p10 and p12 subunits of caspase-8 were not recognized by our anti-caspase-8 antibody. As the so-called caspase-8 specific substrate IETD-AMC can also be cleaved by other caspases [42], including caspase-3, we decided to determine caspase-8 activity by the cleavage of its major substrate Bid by western blotting instead of a fluorogenic IETDase assay.

As shown in Fig. 3a, p55 caspase-8 was cleaved into p43 after 2 h of FasL treatment while the production of the second cleavage product, p18, was slightly delayed. The presence of AB06 did not prevent p43 formation, but entirely blocked the generation of p18. In fact, p43 even slightly accumulated, indicating that it could not be further processed to p18 due to a block in caspase-3 activity. The less potent caspase-3/-7 inhibitor AB13 still allowed the formation of some p18 suggesting that p18 caspase-8 formation correlated with the amount of active p17 caspase-3 levels.
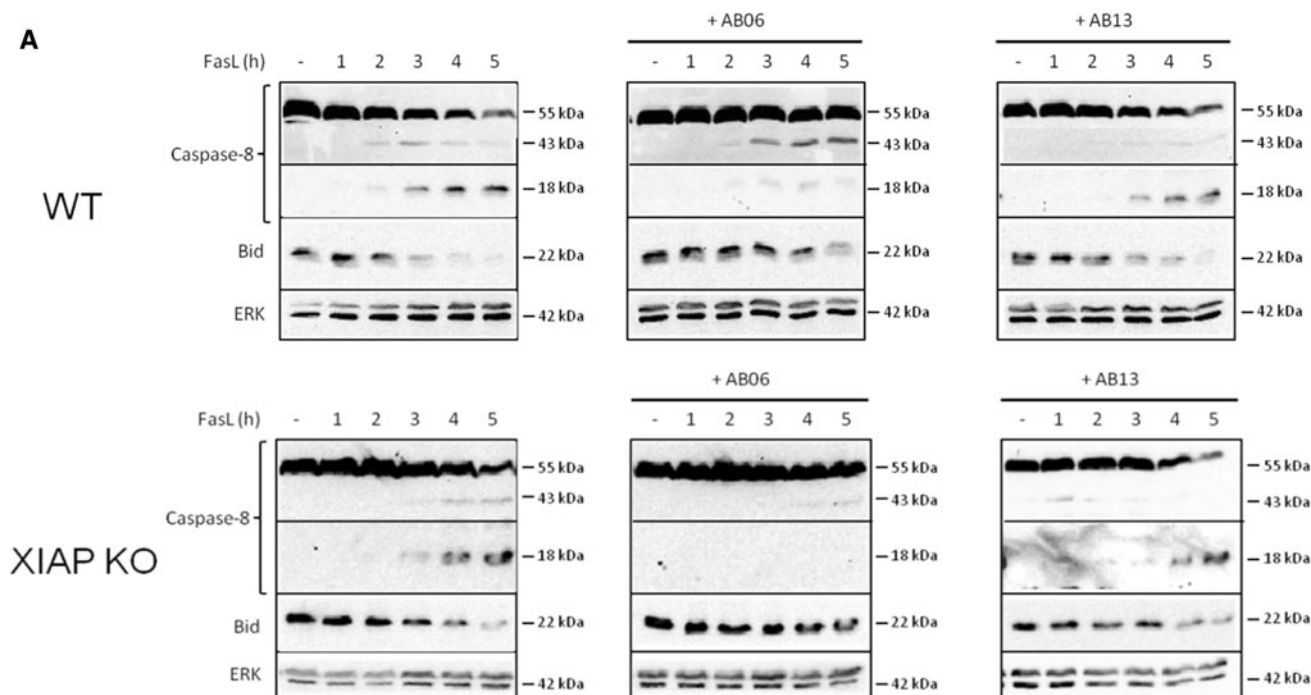
Fig. 3 The formation of p18 caspase-8 and Bid cleavage are dependent on caspase-3 activity. **a** Anti-caspase-8 and anti-Bid western blots of whole cell lysates of wt and XIAP$^{-/-}$ (KO) primary mouse hepatocytes challenged with 100 ng/ml N2A FasL in the absence or presence of 1 μM of the caspase-3 AB06 or AB13 for up to 5 h. 42 kDa ERK served as loading control. The molecular masses of the respective protein bands are indicated on the right of the blots. Note that in the presence of AB06 no p18 caspase-8 is formed and Bid is stabilized. AB13 had only partial effects. Light intensity

quantification of **b** the p55, p43 and p18 caspase-8 (C3) and **c** the p22 full length Bid bands from 3 to 8 independent experiments (*n*) of which one is represented in **a**. Values are depicted in Boehringer light units (BLU). The data were processed by asinh-transformation, normalized to the same average and shifted to a common initial data point ($t_0 = 0$) as described in "Experimental procedures". The mean of at least 3 independent experiments is shown with standard errors. Please note that ordinates for wt and XIAP KO are not the same
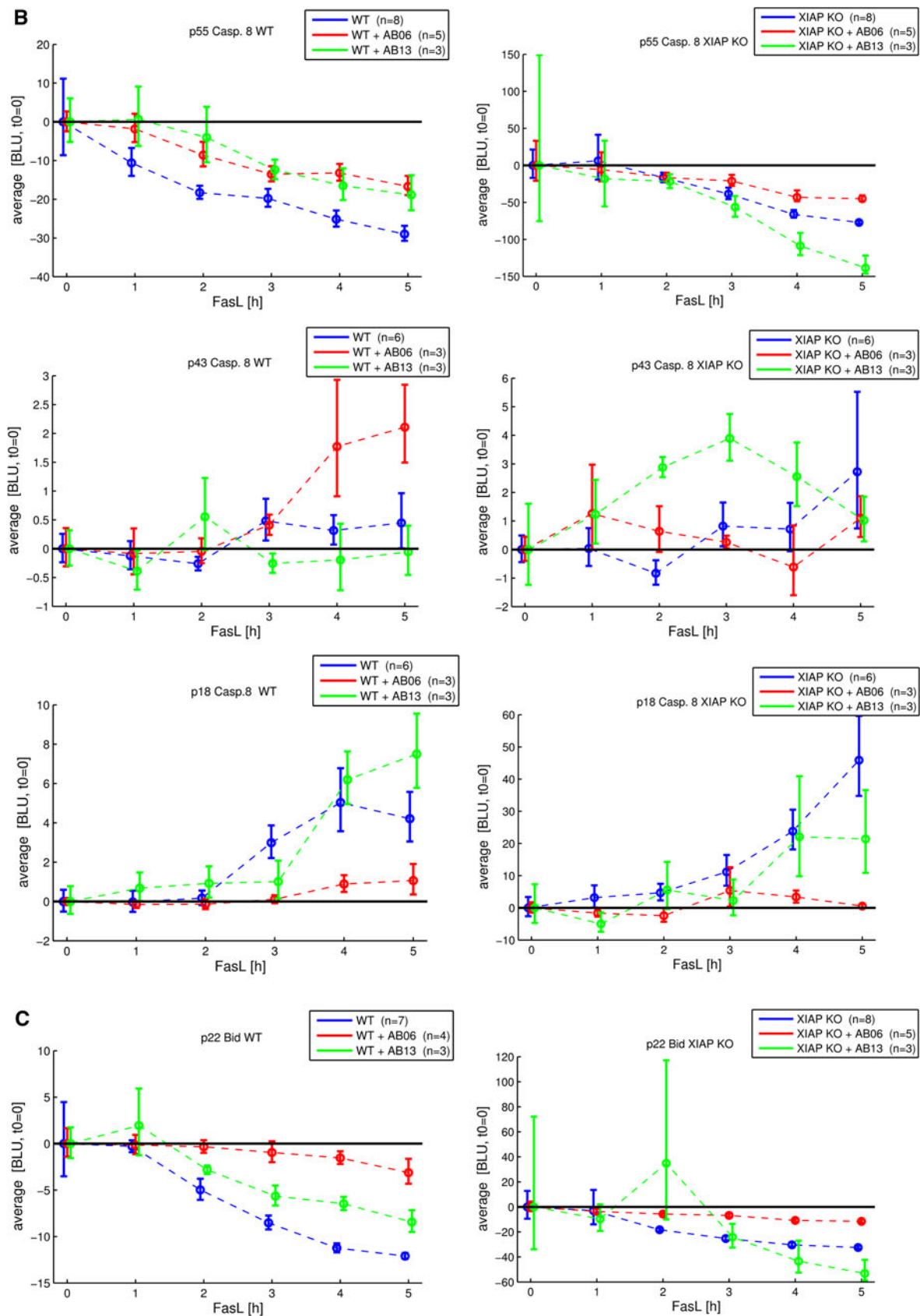
Fig. 3 continued

In XIAP$^{-/-}$ hepatocytes, we noted a higher amount of p18 caspase-8 with time of FasL treatment (Fig. 3a). This would be expected if, due to the lack of XIAP, increased caspase-3 activity cleaved p43 more rapidly into p18. As in wt cells, AB06 entirely blocked the formation of p18 while some p18 was still generated in the presence of AB13. These data clearly show that p18 formation depends on caspase-3 activity.

Unfortunately, we were unable to correlate the formation of the p43 and/or p18 forms of caspase-8 with the cleavage of its major substrate Bid. As expected, in FasL-treated wt and XIAP$^{-/-}$ hepatocytes, the disappearance of full length p22 Bid (and the consequent formation of p15 tBid, not shown) correlated with p43 and p18 formation (after 2–3 h of FasL addition) (Fig. 3a). However, in the presence of AB06, where p43 accumulated and caspase-8 activity should be higher, less Bid was proteolyzed. On the other hand, Bid was similarly cleaved in AB13 treated as compared to untreated cells. We speculate that this discrepancy was due to the fact that Bid is not only a good substrate for caspase-8, but also for caspase-3 [35, 36]. Thus, as for p18 caspase-8 formation, cleavage of Bid was dependent on caspase-3 activity levels (Fig. 3a).

Again quantification of the luminescent caspase-8 bands of 3–8 experiments by Lumi Imager^{TM} (Fig. 3b, c) confirmed the data shown by the representative western blots in Fig. 3a. In general, little p43 caspase-8 was detected in response to FasL, presumably because little active caspase-8 is needed to transmit the apoptotic signal and/or because p43 is further converted to p18. This was especially true in XIAP$^{-/-}$ cells where p43 levels were so low that their quantitation greatly varied and was barely above background/noise (Fig. 3b). By contrast, p18 caspase-8 gradually accumulated after 3 h of FasL treatment, the upregulation was more pronounced in XIAP$^{-/-}$ cells and fully inhibited by AB06, but only partially by AB13 (Fig. 3b—note that the ordinates for XIAP KO are higher than for wt). Moreover, the disappearance of the full-length p22 Bid molecule due to proteolysis correlated with the levels of caspase-3 activity (Fig. 3c).

In summary, our data show that while the formation of the active p43 caspase-8 fragment is due to autoprocessing of clustered p55 procaspase-8 molecules, p18 caspase-8 formation largely depends on caspase-3 activity in FasL-treated primary hepatocytes dying via the direct type I signaling pathway. We could therefore confirm the mathematical model by Eissing et al. [31] that caspase-3 feeds back on caspase-8 to further process p43 caspase-8 to a p18 form. Moreover, we show that caspase-3 triggers the proteolysis of Bid either directly or indirectly by enhancing caspase-8 activation. It also downregulates its own inhibitor XIAP.

Caspase-3 to caspase-8 feedback loop: is it further enhancing caspase-3 activity (positive) or downregulating caspase-8 activity (negative)?

The question remained. What is the physiological significance of this caspase-3 to caspase-8 feedback loop in the type I FasL signaling pathway for apoptosis? One possibility is that p18 is a highly active form of caspase-8, which processes more p32 procaspase-3 into p19/p17 active caspase-3 (positive feedback). As shown in Fig. 1b, caspase-3 processing and activity further increase during the formation of p18 caspase-8 formation in both wt and XIAP$^{-/-}$ cells (between 3 and 5 h of FasL treatment) indicating that p18 could positively influence caspase-3 activity and thereby accelerate FasL-induced apoptosis (Fig. 4a). Alternatively, p18 may just be a degradation product of p43 that does not further cleave p32 procaspase-3 as a substrate (negative feedback) or is directed towards other, not yet identified substrates implicated in the recently published, pleiotropic effects of caspase-8 (Fig. 4b). We cannot distinguish between these two possibilities because
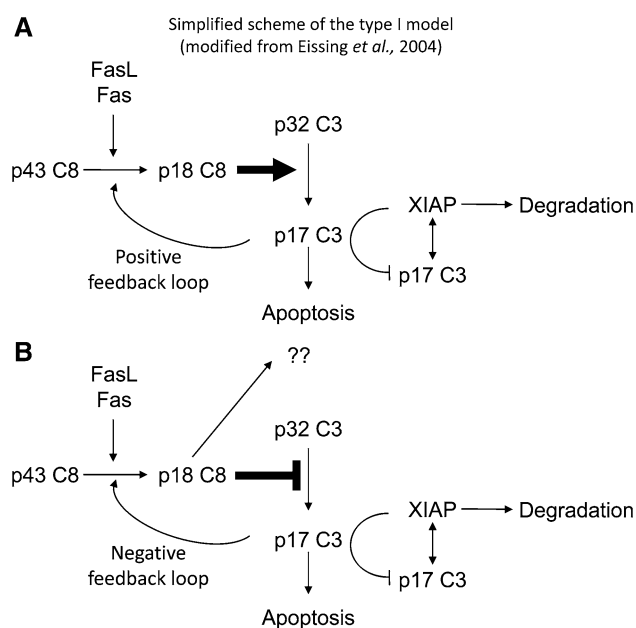
Fig. 4 Simplified scheme of the type I apoptotic pathway (modified from Eissing et al. [31]) in which p17 caspase-3 feeds back to p18 caspase-8. **a** Putative positive feedback loop by which the p18 caspase-8 (C8) generated by proteolysis from p17 caspase-3 (C3) further enhances p32 to p17 C3 processing and thereby accelerates apoptosis **b** Putative negative feedback loop by which the p18 caspase-8 (C8) generated by proteolysis from p17 caspase-3 (C3) shuts down p32 to p17 C3 processing, thereby restricting apoptosis. Alternatively, p18 caspase-8 may target others yet unknown substrates implicated in non-apoptotic processes of FasL signaling (question marks). While our data shown here cannot distinguish between a positive or negative feedback loop, we can show that p17 C3 also degrades its own inhibitor XIAP, thereby enhancing caspase-3 activation and apoptosis in a positive manner

no specific inhibitor against p18 caspase-8 is available which does not also affect caspase-3. However, recent data from other laboratories suggested that p18 formation diminishes rather than enhances FasL-induced apoptosis (see "Discussion" below).

Discussion

A mathematical model developed by Eissing et al. [31] predicted that a positive feedback loop between caspase-3 and caspase-8 activation caused bistability of the type I and type II signaling cascades induced by FasL. We used here two caspase-3/-7 specific inhibitors and genetic deletion of the major endogenous caspase-3 inhibitor XIAP to show that in type I FasL signaling of primary mouse hepatocytes, such a caspase-3 to caspase-8 feedback loop indeed exists, but its impact cannot be estimated until we have access to better tools (such as specific caspase-8 inhibitors) and quantified kinetic data.

In FasL signaling, p55/p53 pro-caspase-8a/b are rapidly recruited to the DISC, triggering the autoprocessing of the initiator caspase into p43/p41 and p10/p12 fragments which form active tetrameric p43/p12 and p41/p10 complexes at the DISC. As recently shown, this autoprocessing is absolutely required for apoptosis signaling, either by directly processing p32 procaspase-3 into active p19 and p17 fragments or by cleaving Bid which activates caspase-3 via Bax/Bak mediated MOMP, cytochrome c release and Apaf-1/caspase-9 apoptosome formation [20, 24, 26]. We do not know if primary hepatocytes express both p55 caspase-8a and p53 caspase-8b. It seems that we detect only one band for both the p55/p53 proforms as well as the p43/p41 autoprocessed forms. We however consistently see autoprocessing of caspase-8 in response to FasL treatment, which is concomitant in time with the processing of p32 pro-caspase-3 into p19 and p17. Most importantly, 1 μM of the highly selective, potent caspase-3/-7 inhibitor AB06 blocks not only p19 to p17 caspase-3 processing, caspase-3/-7 DEVDase activity and apoptosis, but also the further cleavage of the DISC-associated p43 to a cytosolic p18 caspase-8 fragment. As the autoprocessing of p43 is not affected by this inhibition, it is clear that AB06 does not block caspase-8 activity. Indeed, Berger et al. [38] showed that the Ki(app) of AB06, the value for the speed of the inhibitor binding to the target enzyme, was 250 times higher for caspase-3 than for caspase-8. In the same study, it was reported that 10 μM of AB06 or AB13 cross-inhibited other caspases, including caspase-8, whereas 1 μM was specific for caspases-3 and -7 [38]. In addition, in XIAP$^{-/-}$ cells where more caspase-3 activity and processing is detected, the levels of p18 caspase-8 increase and this enhancement is also fully blocked by

AB06. As we performed the western blot experiments up to 8 times, accurately quantified the caspase-3 and -8 bands by luminescence measurements and ensured the specificity of the inhibitors by using a final concentration of 1 μM, we can be confident that the processing of p43 to p18 caspase-8 is a caspase-3 dependent feedback event. The caspase-3/-7 inhibitor AB13 turned out to be less potent in blocking caspase-3/-7 activity, most likely because it did not effectively interact with p19 (no band shift, see Fig. 2a) and hence could not entirely block its autoproteolysis to p17. However, AB13 was as efficient as AB06 in inhibiting the enzymatic activity of p17 (Fig. 1b) and by consequence the proteolysis of PARP, Bid as well as XIAP (Fig. 2a, c). Our data are consistent with Berger et al. [38], showing that AB13 binds about 2 times slower to caspase-3 than AB06.

What is the significance of the caspase-3 to caspase-8 feedback loop for FasL-induced apoptosis? Such a loop has been predicted by Systems Biology simulations in the type I SKW6.4 and the type II HeLa cells using XIAP as caspase-3 and BAR (bifunctional apoptosis regulator) as caspase-8 inhibitor [43]. However, neither one of these two inhibitors were selective for the respective caspases and thus experimental proof of such a feedback loop has been so far missing. Moreover, although the mathematical modeling suggested a positive feedback loop in both cases (type I and type II), it could not been proven that a further processing of the p43 or p41 caspase-8 to p18 indeed accelerated caspase-3 activation and apoptosis. Recently, Hughes et al. [24] and Oberst et al. [26] generated caspase-8 mutants, which could still be auto-processed to the p43, but not to p18. (D216A/D210A). Surprisingly, these mutants were even more potent in processing and activating caspase-3 and inducing apoptosis than the wild-type forms suggesting that p18 formation was either an apoptosis down-regulating event or a means to direct p18 caspase-8 towards another substrate than Bid or caspase-3. Caspase-8 has been implicated in a variety of other cellular processes such as cell proliferation and differentiation [19–22]. However, mice carrying knock-in caspase-8 mutants revealed that it was the clustered, non-processed p55/p53 rather than the fully processed p18 form of caspase-8, which was responsible for these non-apoptotic effects [20]. It is therefore still unclear, what substrates and signaling pathways are affected by p18 caspase-8 and the significance of the caspase-3 to caspase-8 feedback loop described herein remains to be identified.

By contrast, we obtained good evidence from our analysis that caspase-3 could amplify type I FasL signaling through the cleavage of Bid and the degradation of its own inhibitor XIAP. In type II signaling, XIAP is neutralized by the release of Smac/DIABLO and other apoptogenic factors [17]. These factors bind to XIAP and prevent its interaction with caspase-9 and caspase-3. Like this, both caspases can be fully activated and the apoptotic signaling through mitochondria is accelerated. In type I signaling, the release of apoptogenic factors

from mitochondria is not detectable and hence another mechanism has to prevail in order to eliminate XIAP and enhance apoptosis signaling through caspase-3. Based on our data that XIAP degradation is blocked by AB06 and AB13, together with structural evidence that caspase-3 binds to XIAP's BIR2 domain [44] and both proteins co-immunoprecipitate hepatocyte lysates [45], we propose that in type I FasL signaling low levels of p17 caspase-3 cleave and neutralize XIAP, thereby increasing caspase-3 activity and consequent apoptosis with time. With regard to the cleavage of Bid by caspase-3, it is not clear if this really constitutes a positive feedback loop. It was very difficult to detect the tBid cleavage fragment by our antibody and in fact, not much of tBid is needed to trigger Bax/Bak-mediated MOMP [46]. Thus, we cannot say if caspase-3-mediated cleavage of Bid leads to type II, mitochondrial apoptosis amplification loop rather than a simple degradation and inactivation of Bid. Further experiments with caspase-3 cleavage mutants of XIAP and BID will unveil the significance of these feedback loops for type I FasL induced apoptosis signaling. Moreover, the development of a mathematical model connecting caspase-3 with Bid and XIAP will shed more light on these mechanisms.

Our data show how in silico models can be used to predict biological outcome of complex signaling events. However, we still need optimal tools, such as the caspase-3/-7 specific inhibitors AB06 and AB13 and XIAP deletion to prove that the prediction is right. Even then more mathematical models and experimental tools are required to identify the significance of the feedback loops and crosstalks implicated in these complex signaling systems.

Conflict of interest The authors declare that they have no conflict of interest.

References

1. Meier P, Finch A, Evan G (2000) Apoptosis in development. Nature 407:796–801
2. Kanzler S, Galle PR (2000) Apoptosis and the liver. Semin Canc Biol 10:173–184
3. Osagawara J, Watanabe-Fukunaga R, Adachi M, Matsuzawa A, Kasugai T, Kitamura Y, Itoh N, Suda T, Nagata S (1993) Lethal effect of the anti-Fas antibody in mice. Nature 364:806–809
4. Galle PR, Krammer PH (1998) CD95-induced apoptosis in human liver disease. Semin Liver Dis 18:141–151
5. Canbay A, Friedman S, Gores GJ (2004) Apoptosis: the nexus of liver injury and fibrosis. Hepatology 39:273–278
6. Ni R, Tomita Y, Matsuda K, Ichihara A, Ishimura K, Ogasawara J, Nagata S (1994) Fas-mediated apoptosis in primary cultured mouse hepatocytes. Exp Cell Res 215:332–337
7. Schüngel S, Buitrago-Molina LE, devi Nalapareddy P, Lebofsky M, Manns MP, Jaeschke H, Gross A, Vogel A (2009) The strength of the Fas ligand signal determines whether hepatocytes act as type 1 or type 2 cells in murine livers. Hepatology 50:1558–1566
8. Yin XM, Wang K, Gross A, Zhao Y, Zinkel S, Klocke B, Roth KA, Korsmeyer SJ (1999) Bid-deficient mice are resistant to Fas-induced hepatocellular apoptosis. Nature 400:886–891
9. Kaufmann T, Tai L, Ekert PG, Huang DCS, Norris F, Lindemann RK, Johnstone RW, Dixit VM, Strasser A (2007) The BH3-only protein Bid is dispensable for DNA damage- and replicative stress-induced apoptosis or cell-cycle arrest. Cell (129):423–433
10. Scaffidi C, Fulda S, Srinivasan A, Friesen C, Li F, Tomaselli KJ, Debatin KM, Krammer PH, Peter ME (1998) Two CD95 (APO-1/Fas) signaling pathways. EMBO J 17:1675–1687
11. Peter ME, Krammer PH (2003) The CD95(APO-1/Fas) DISC and beyond. Cell Death Differ 10:26–35
12. Chang DW, Xing Z, Capacio VL, Peter ME, Yang X (2003) Interdimer processing mechanism of procaspase-8 activation. EMBO J 22:4132–4142
13. Medema JP, Scaffidi C, Kischkel FC, Schevchenko A, Mann M, Krammer PH, Peter ME (1997) FLICE is activated by association with the CD95 death-inducing signaling complex (DISC). EMBO J 16:2794–2804
14. Muzio M, Stockwell BR, Stennicke HR, Salvesen GS, Dixit VM (1998) An induced proximity model for caspase-8 activation. J Biol Chem 273:2926–2930
15. Gross A, Yin XM, Wang K, Wei MC, Jockel J, Milliman C, Erdjument-Bromage H, Tempst P, Korsmeyer SJ (1999) Caspase cleaved BID targets mitochondria and is required for cytochrome c release, while Bcl-xL prevents this release but not tumor necrosis factor-R1/Fas death. J Biol Chem 274(2):1156–1163
16. Peter ME, Budd RC, Desbarats J, Hedrick SM, Hueber AO, Newell MK, Owen LB, Pope RM, Tschopp J, Wajant H, Wallach D, Wiltrout RH, Zörnig M, Lynch DH (2007) The CD95 receptor: apoptosis revisited. Cell 129:447–450
17. Green DR, Kroemer G (2004) The pathophysiology of mitochondrial cell death. Science 305:626–629
18. Desbarats J, Newell MK (2000) Fas engagement accelerates liver regeneration after partial hepatectomy. Nat Med 6:920–923
19. Kang TB, Ben-Moshe T, Varfolomeev EE, Pewzner-Jung Y, Yogev N, Jurewicz A, Waisman A, Brenner O, Haffner R, Gustafsson E, Ramakrishnan P, Lapidot T, Wallach D (2004) Caspase-8 serves both apoptotic and nonapoptotic roles. J Immunol 173:2976–2984
20. Kang TB, Oh GS, Scandella E, Bolinger B, Ludewig B, Kovalenko A, Wallach D (2008) Mutation of a self-processing site in caspase-8 compromises its apoptotic but not its nonapoptotic functions in bacterial artificial chromosome-transgenic mice. J Immunol 181:2522–2532
21. Barbero S, Mielgo A, Torres V, Teitz T, Shields DJ, Mikolon D, Bogyo M, Barilà D, Lahti JM, Schlaepfer D, Stupack DG (2009) Caspase-8 association with the focal adhesion complex promotes tumor cell migration and metastasis. Cancer Res 69(9):3755–3763
22. Kovalenko A, Kim JC, Kang TB, Rajput A, Bogdanov K, Dittrich-Breiholz O, Kracht M, Brenner O, Wallach D (2009)

Caspase-8 deficiency in epidermal keratinocytes triggers an inflammatory skin disease. J Exp Med 206:2161–2177

23. Keller N, Mares J, Zerbe O, Grütter MG (2009) Structural and biochemical studies on procaspase-8: new insights on initiator caspase activation. Structure 17:438–448

24. Hughes MA, Harper N, Butterworth M, Cain K, Cohen GM, MacFarlane M (2009) Reconstitution of the death-inducing signaling complex reveals a substrate switch that determines CD95-mediated death or survival. Mol Cell 35:265–279

25. Strasser A, Jost PJ, Nagata S (2009) The many roles of FAS receptor signaling in the immune system. Immunity 30:180–192

26. Oberst A, Pop C, Tremblay AG, Blais V, Denault JB, Salvesen GS, Green DR (2010) Inducible dimerization and inducible cleavage reveal a requirement for both processes in caspase-8 activation. J Biol Chem 285(22):16632–16642

27. Blanc C, Deveraux QL, Krajewski S, Jänicke RU, Porter AG, Reed JC, Jaggi R, Marti A (2000) Caspase-3 is essential for procaspase-9 processing and cisplatin-induced apoptosis of MCF-7 breast cancer cells. Cancer Res 60:4386–4390

28. Fujita E, Egashira J, Urase K, Kuida K, Momoi T (2001) Caspase-9 processing by caspase-3 via a feedback amplification loop in vivo. Cell Death Differ 8:335–344

29. Slee EA, Harte MT, Kluck RM, Wolf BB, Casiano CA, Newmeyer DD, Wang HG, Reed JC, Nicholson DW, Alnemri ES, Green DR, Martin SJ (1999) Ordering the cytochrome c-initiated caspase cascade: hierarchical activation of caspases-2, -3, -6, -7, -8, and -10 in a caspase-9-dependent manner. J Cell Biol 144(2):281–292

30. Van de Craen M, Declercq W, Van den brande I, Fiers W, Vandenabeele P (1999) The proteolytic procaspase activation network: an in vitro analysis. Cell Death Differ 6:1117–1124

31. Eissing T, Conzelmann H, Gilles ED, Allgöwer F, Bullinger E, Scheurich P (2004) Bistability analyses of a caspase activation model for receptor-induced apoptosis. J Biol Chem 279(35):36892–36897

32. Angeli D, Ferrell JE, Sontag ED (2004) Detection of multistability, bifurcations, and hysteresis in a large class of biological positive-feedback systems. Proc Natl Acad Sci USA 101(7):1822–1827

33. Ferrell JE (2002) Self-perpetuating states in signal transduction: positive feedback, double-negative feedback and bistability. Curr Opin Cell Biol 14(2):140–148

34. Legewie S, Blüthgen N, Herzel H (2006) Mathematical modeling identifies inhibitors of apoptosis as mediators of positive feedback and bistability. PLoS Comput Biol 2(9):e120

35. Tang D, Lahti JM, Kidd VJ (2000) Caspase-8 activation and Bid cleavage contribute to MCF7 cellular execution in a caspase-3-dependent manner during staurosporine-mediated apoptosis. J Biol Chem 275(13):9303–9307

36. Slee EA, Keogh SA, Martin SJ (2000) Cleavage of BID during cytotoxic drug and UV radiation-induced apoptosis occurs downstream of the point of Bcl-2 action and is catalyzed by caspase-3: a potential feedback loop for amplification of apoptosis-associated mitochondrial cytochrome c release. Cell Death Differ 7:556–565

37. Walter D, Schmich K, Vogel S, Pick R, Kaufmann T, Hochmuth FC, Haber A, Neubert K, McNelly S, von Weizsäcker F, Merfort I, Maurer U, Strasser A, Borner C (2008) Switch from type II to I Fas/CD95 death signaling on in vitro culturing of primary hepatocytes. Hepatology 48:1942–1953

38. Berger AB, Witte MD, Denault JB, Sadaghiani AM, Sexton KMB, Salvesen GS, Bogyo M (2006) Identification of early intermediates of caspase activation using selective inhibitors and activity-based probes. Mol Cell 23:509–521

39. Klingmüller U, Bauer A, Bohl S, Nickel PJ, Breitkopf K, Dooley S et al (2006) Primary mouse hepatocytes for systems biology approaches: a standardized in vitro system for modelling of signal transduction pathways. Syst Biol (Stevenage) 153:433–447

40. Shimizu M, Fontana A, Takeda Y, Yagita H, Yoshimoto T, Matsuzawa A (1999) Induction of antitumor immunity with Fas/APO-1 ligand (CD95L)-transfected neuroblastoma Neuro-2a cells. J Immunol 162:7350–7357

41. Huber W, von Heydebreck A, Sültmann H, Poustka A, Vingron M (2002) Variance stabilization applied to microarray data calibration and to the quantification of differential expression. Bioinformatics 18(Suppl 1):S96–S104

42. Pop C, Salvesen GS (2009) Human caspases: activation, specificity, and regulation. J Biol Chem 284(33):21777–21781

43. Würstle ML, Laussmann MA, Rehm M (2010) The caspase-8 dimerization/dissociation balance is a highly potent regulator of caspase-8, -3, -6 signaling. J Biol Chem 285(43):33209–33218

44. Eyrisch S, Medina-Franco JL, Helms V (2011) Transient pockets on XIAP-BIR2: toward the characterization of putative binding sites of small-molecules XIAP inhibitors. J Mol Model. doi: 10.1007/s00894-011-1217-y

45. Jost PJ, Grabow S, Gray D, McKenzie MD, Nachbur U, Huang DCS, Bouillet P, Thomas HE, Borner C, Silke J, Strasser A, Kaufmann T (2009) XIAP discriminates between type I and type II FAS-induced apoptosis. Nature 460(20):1035–1039

46. Madesh M, Antonsson B, Srinivasula SM, Alnemri ES, Hajnóczky G (2002) Rapid kinetics of tBid-induced cytochrome c and Smac/DIABLO release and mitochondrial depolarization. J Biol Chem 277(7):5651–5659